Effects of water vapour addition to the air stream on soot volume fraction and flame temperature in a laminar coflow ethylene flame

Liu, Fengshan; Consalvi, Jean-Louis; Fuentes, Andrés; Smallwood, Gregory J.

Publisher's version / Version de l'éditeur:
https://doi.org/10.1615/ICHMT.2013.IntSympRadTransf.90
Proceedings of the 7th International Symposium on Radiative Transfer, RAD-13, 2013-06-08

NRC Publications Record / Notice d'Archives des publications de CNRC:
https://nrc-publications.canada.ca/eng/view/object/?id=bd1a93ec-e4c9-49a7-8d53-20ab8c016496
https://publications-cnrc.canada.ca/fra/voir/objet/?id=bd1a93ec-e4c9-49a7-8d53-20ab8c016496

Proceedings of the 7th International Symposium on Radiative Transfer, RAD-13
June 2-8, 2013, Kuşadasi, Turkey

RAD-13-XX

EFFECTS OF WATER VAPOUR ADDITION TO THE AIR STREAM ON SOOT VOLUME FRACTION AND FLAME TEMPERATURE IN A LAMINAR COFLOW ETHYLENE FLAME

Fengshan Liu[*], Jean-Louis Consalvi[**], Andrés Fuentes[***], and Gregory J. Smallwood[*]
[*]National Research Council Canada,
Building M-9, 1200 Montreal Road, Ottawa, ON, Canada K1A 0R6
[**]Aix-Marseille Université, IUSTI/ UMR CNRS 7343,
5 rue E. Fermi, 13453 Marseille Cedex 13, France
[***]Departamento de Industrias, Universidad Técnica Federico Santa María,
Av. España 1680, Valparaíso, Chile

ABSTRACT. The effects of adding water vapour to the air stream on flame temperature and soot volume fraction were investigated numerically in a laminar coflow ethylene diffusion flame at atmospheric pressure using a detailed C2 reaction mechanism including PAH. Thermal radiation was calculated using the discrete-ordinates method and a statistical narrow-band correlated-k based wide band model for the absorption coefficients of CO_2 and H_2O. Soot formation was modeled using a PAH based inception model and the HACA mechanism for surface growth and oxidation. The added water vapour affects soot formation and flame properties through not only dilution and thermal effects, but also through chemical and radiation effects. Addition of water vapour significantly reduces radiation heat loss.

INTRODUCTION

Understanding the effects of water vapour addition to the oxidizer stream of a diffusion flame is of fundamental interest and great practical importance to combustion applications, such as NO_x emission control [1,2] and fire suppression [3-5]. When water mist is added to a fire or flame it causes extinction through the mechanisms of gas-phase cooling, oxygen dilution, and radiation attenuation [3]. Lentati and Chelliah categorized the effects of water mist on flames as (1) physical effects due to water droplet size, which affects the trajectory and evaporation process of the droplet, (2) thermal effects due to heat capacity and latent heat of evaporation, and (3) chemical effects due to enhanced overall three-body recombination reactions and shift in water-gas reactions [6].

It has generally been thought that water suppresses combustion processes mainly through physical mechanisms, i.e., dilution and thermal capacity, in both planar premixed flames [7] and counterflow diffusion flames [5,6] by reducing the flame temperatures and dilution of the reactants. These studies found that the direct chemical effects of water vapour on the laminar burning velocity or the extinction strain rate are quite small. Thermal radiation transfer was neglected in these studies and hence the role of radiation absorption by the added water vapour or water droplets was not evaluated. The chemical effects of water vapour on flame temperature, burning velocity, and soot and CO formation in premixed flames and diffusion flame have been demonstrated by Müller-Dethlefs and Schlander [8] and Richard et al. [9], respectively.

Although most studies on the effectiveness and mechanisms of water mist suppression of flames were performed experimentally, several numerical studies have also been conducted. Lentati and Chelliah [5]

carried out numerical studies of the dynamics of water droplets in counterflow methane/air diffusion flames. They found that the optimal droplet sizes for flame suppression are between 20 to 30 μm. Prasad et al. [10] modeled the interactions between water mist and a coflow laminar methane-air diffusion flame established on a Wolfhard-Parker slot burner by solving the full Navier-Stokes (NS) equations. The focus of their study was the effect of droplet size on the extinction water concentration. Ananth and Mowrey conducted a numerical investigation of the interactions between ultra-fine water mist and an axisymmetric laminar coflow propane diffusion flame by solving the unsteady NS equations [4]. Chemical reactions were modeled using the GRI-3.0 reaction mechanism. Soot formation was neglected because their main concerns were the water droplet size effect and the extinction conditions. Thermal radiation transfer was calculated using the P_1-approximation and the weighted-sum-of-gray-gases model. The emphasis of the study of Ananth and Mowrey [4] was the extinction conditions, not the interactions of water vapour with soot formation and radiation absorption.

The numerical studies on combustion suppression using water mist focused on the dynamics of water droplets in the combustion flow field. Nevertheless, little attention has been paid to the chemical effects of water vapour on soot formation and other flame properties in spite of the fact that the experimental work of Richard et al. [9], who demonstrated that addition of water vapour to a heptane pool fire inhibits chemically the soot formation process. The chemical effects of water vapour were investigated numerically by Suh and Atreya [11] by substituting nitrogen in the oxidizer stream by water vapour and argon while keeping the oxygen concentration constant in counterflow methane diffusion flame. They showed that addition of water vapour to the oxidizer stream increases the flame temperature and promotes OH radical concentration, which in turn lowers CO concentration and enhances CO_2 concentration. The pathways for the chemical effect of H_2O, however, were not identified.

Comprehensive models for flame/fire interaction with water mist have also in general neglected the radiation absorption/attenuation effect by water droplets and water vapour, although the potential importance of such effect has been noticed by Tseng and Viskanta [12], Yang et al. [13], and Consalvi et al. [14]. The objective of this study is to understand the chemical and radiation absorption effects of water vapour added to the oxidizer stream of a laminar coflow ethylene/air diffusion flame. Combustion chemistry was modeled using a detailed mechanism for C_2 hydrocarbon fuels. To account for the radiation absorption effect of the added water vapour and radiation heat transfer in the flame the radiative properties of radiating species, namely CO, CO_2, and H_2O were modeled using a statistical narrow-band correlated-k based wide-band model. The potential chemical effect of the added water vapour on soot formation was investigated using a sophisticated soot formation model based on polycyclic aromatic hydrocarbon (PAH) collision for soot particle inception and the hydrogen abstraction carbon addition (HACA) mechanism for surface growth and oxidation.

NUMERICAL MODEL

The diffusion flames to be modeled in this study are the axisymmetric, atmospheric-pressure, laminar coflow ethylene ones established in the Gülder burner [15] without and with water vapour addition to the oxidizer stream. The burner consists of an inner diameter fuel tube of 10.9 mm (0.94 mm thickness) surrounded by an 88 mm inner diameter annular air tube.

Governing equations The governing equations to be solved in this study are the steady-state fully-coupled elliptic conservation equations for mass, momentum, energy, and species mass fractions in axisymmetric cylindrical coordinates, in the low Mach number limit. These equations have been described in detail in previous studies, e.g., Guo et al. [16], and will not be repeated here. It is worth pointing out that the gravity term is included in the momentum equations and the source term due to thermal radiation transfer is accounted for in the energy equation.

Radiation model The radiation model has also been well documented in the literature, e.g., Liu et al. [17]. The radiative properties of radiating gases, namely CO, CO_2, and H_2O, were modeled using an optimized 9-band model based on the lumping strategy and the statistical narrow-band correlated-k method [18]. The total radiation intensity over each spectral band is evaluated using the 4-point Gauss-Legendre quadrature scheme. The absorption coefficients at each quadrature point and each band were precalculated and fit as a polynomial function of temperature [18]. The absorption coefficient of soot was calculated using the Rayleigh expression as $k_s = 5.5 f_v \eta_c$ with f_v being the soot volume fraction and η_c the wavenumber at the band centre. The radiative transfer equation in 2D axisymmetric cylindrical coordinates was solved by the discrete-ordinates method described in detail in [17].

Soot model Since the acetylene based two-equation soot model is in general unable to predict the chemical effects on soot formation, it is necessary to employ a more sophisticated soot formation model to investigate the chemical effect of the added water vapour on the flame properties and soot formation. The soot model employed in this study has been described in detail in Zhang et al. [19] and is only briefly summarized below.

Soot inception was assumed to be the result of collision of two pyrene molecules (A4). The subsequent surface growth and oxidation were assumed to follow the HACA mechanism [20]. The aggregation process of soot particles was modeled using a sectional model [19]. In the sectional model each aggregate is assumed to be compromised of equally sized spherical primary particles and to have the same fractal dimension of 1.8. The mass range of aggregates is divided into a number of discrete sections with prescribed masses. Soot aggregates are assigned into these prescribed sections according to their mass. The nucleation step connects the gaseous incipient species (A4) with the solid phase. The sectional transport equations for soot aggregates and primary particles can be found in [19].

Soot nucleation rate is calculated by the collision rate of two pyrene molecules in the free-molecular regime, but enhanced by a factor of 2.2 due to van der Waals force [21]. Surface growth and oxidation rates are calculated by the HACA mechanism described in [20]. PAH condensation on soot particles contributes to the surface growth of soot due to the condensation. This process is modeled by the collision of pyrene molecules with soot aggregates. The condensation rate is calculated by the collision theory between pyrene molecules and aggregates [22]. Since not all collisions lead to successful condensation, the A4-soot collisional condensation efficiency is assumed to be 0.5. In this study, 35 sections were used in the sectional model with a spacing factor of 2.35 [19]. The capability of the soot model to predict soot volume fractions and to capture the dynamic of soot particles in laminar coflow ethylene flames has been demonstrated in Zhang et al. [19].

Chemical kinetic mechanism The reaction kinetics of ethylene was modeled using the mechanism of Appel et al. [20], which was primarily developed for C_2 hydrocarbons with PAH formation. This mechanism consists of 101 species and 544 reactions with PAH formation and growth up to A4.

Numerical method The numerical methods have been described in several previous publications. Only a brief summary is provided here. The governing equations are discretized by the standard finite volume method. The classical SIMPLE algorithm with the staggered mesh is used to handle the pressure and velocity coupling [23]. The diffusive terms are discretized by the second order central difference scheme while the convective terms are discretized by the power law scheme [23]. The gaseous species equations are solved simultaneously to effectively deal with the stiffness of the system and speedup the convergence process [24]. The sectional soot equations are solved in the same manner as the species equations due to the stiffness of the system. The remaining governing

equations are solved by the Tri-Diagonal Matrix Algorithm. The thermal and transport properties of gaseous species and chemical reaction rates are obtained by CHEMKIN subroutines [25] and the database associated with the Appel et al. reaction mechanism [20]. Since the sectional soot model and the fairly large reaction mechanism in the present 2D flame calculations are very computationally demanding, it is paramount to implement these numerical models in the parallel mode with the domain decomposition method [26]. The whole computational domain is divided uniformly in the z-direction into 16 sub-domains and each sub-domain is assigned to one CPU for the calculation. The algorithm uses the Message Passing Interface (MPI) library of Fortran to parallelize the code.

The boundary conditions have been described in previous studies, e.g. [19, 26]. A parabolic profile was assumed for the inlet velocity of the fuel stream as $u = 2u_F[1-(r/R_I)^2]$, where r is the radial position, R_I is the inner radius of the fuel tube, and u_F is the average velocity of the fuel stream. For the air stream a uniform velocity profile was assigned outside the boundary layer formed at the outer surface of the fuel tube. Inside this boundary layer a boundary layer type velocity profile was assumed. Symmetry, free-slip, and zero-gradient conditions were specified at the centerline, outer radial boundary, and the exit boundary, respectively. The ideal gas state equation was used to calculate the gas density.

RESULTS AND DISCUSSION

All the numerical calculations were conducted in a domain of 10.46 cm (z) × 4.71 cm (r) using 210 (z) × 88 (r) control volumes. A non-uniform mesh was used to save computational time while resolving the large gradients. Very fine grids are placed in the r-direction (resolution 0.2 mm) near the burner exit in the z-direction (resolution 0.3 mm). It was checked that further refinement of the mesh had negligible effects on the results. In all the calculations pure ethylene was delivered to the fuel stream at a temperature of 350 K with an average exit velocity of u_F = 3.4 cm/s. The uniform oxidizer velocity in the baseline case, i.e., without water vapour addition, was assigned at u_O = 50 cm/s. To allow for up to 10% water vapour addition to the oxidizer stream without saturation the oxidizer stream was also preheated to 350 K. When water vapour is added to the oxidizer stream, the oxidizer stream velocity increases according to the amount of water vapour added.

Water vapour is expected to affect soot formation through four mechanisms. The first mechanism is related to the dilution of oxygen which induces modifications in the flame temperature and flame structure. The oxidizer-to-fuel mass ratio is increased and, consequently the adiabatic flame temperature is reduced as water vapour is added to the dry air. Concerning soot production, the resulting decrease in flame temperature is expected to lead to lower rates for soot nucleation and surface growth, and thus to lower soot concentrations. On the other hand, the decreased presence of oxygen and reduced flame temperature inhibit oxidative mechanisms, which tend to increase the soot concentrations. The second mechanism is thermal in nature and is caused by the higher heat capacity of water vapour. The third mechanism is related to the direct chemical effects since water vapour is an active species for the chemical reactions, which alter the concentrations of important species for soot formation, such as H, H_2, C_2H_2, and A4. Finally, the added water vapour participates radiative exchange and contributes to modify flame temperatures and thus soot production and oxidation. It is important to point out that the added water vapour to the oxidizer stream affects flame temperatures radiatively by enhancing emission from the high temperature zones and enhancing the radiative exchange between the hot temperature zones and the cold surroundings.

Eight test cases have been considered to isolate the four mechanisms discussed above. Table 1 summarizes the different compositions of the oxidizer stream for each case. Case 1 represents the

baseline case with an oxidizer stream composed of dry air. In Cases 2 and 5, 5% and 10% of water vapour are added to the dry air, respectively. Cases 3 and 6 are designed to isolate the chemical effects from the dilution effects. A fictitious species named FH_2O was added to the C2 mechanism for this purpose. FH_2O has identical thermal and transport properties as the normal H_2O, but is treated as an inert species, though it is allowed to contribute to the third-body collision processes. To isolate the effect of radiation absorption by the added FH_2O in the oxidizer stream FH_2O is further assumed to be transparent in Cases 4 and 7. Finally, Case 8 was included in the present study to quantify the effect of dilution through a direct comparison between the results of Cases 5 and 8. Iterations in all the calculations conducted in this study were stopped after the maximum relative variation in temperature over 100 iterations was less than 1×10^{-4}.

Table 1: Compositions of the oxidizer stream in the eight cases

Case	Oxidizer stream compositions (mole fraction)	Remark
1	$X_{O2} = 0.209, X_{N2} = 0.791$	Dry air
2	$X_{H2O} = 0.05, X_{O2} = 0.1987, X_{N2} = 0.7513$	H_2O addition
3	$X_{FH2O} = 0.05, X_{O2} = 0.1987, X_{N2} = 0.7513$	Radiating FH_2O addition
4	$X_{FH2O} = 0.05, X_{O2} = 0.1987, X_{N2} = 0.7513$	Non-radiating FH_2O addition
5	$X_{H2O} = 0.1, X_{O2} = 0.1882, X_{N2} = 0.7118$	H_2O addition
6	$X_{FH2O} = 0.1, X_{O2} = 0.1882, X_{N2} = 0.7118$	Radiating FH_2O addition
7	$X_{FH2O} = 0.1, X_{O2} = 0.1882, X_{N2} = 0.7118$	Non-radiating FH_2O addition
8	$X_{O2} = 0.209, X_{N2} = 0.691, X_{H2O} = 0.1$	Replacement of N_2 by H_2O

Temperature and soot volume fraction distributions The distributions of temperature and soot volume fraction for the baseline flame, 10% H_2O addition, and 10% H_2O replacement of N_2 in air are compared in Figs. 1 and 2, respectively. The peak values are also indicated in these figures. For the baseline flame, Fig. 1(a), the stoichiometric flame height (the centerline location where the temperature peaks) is approximately 6 cm. The maximum temperature of 2043.7 K occurs in the annular region low in the flame. Fig. 2(a) shows that soot exhibits the typical behavior observed in buoyant laminar 'candle-like' flames. It is first observed to form in the annular region inside the main reaction zone. The peak of soot within this annulus initially increases with height and then decreases as soot is oxidized higher up in the flame. The present flame is non-smoking, all soot being completely oxidized at the flame tip. As the height increases the location of the peak is shifted toward the axis since soot particles are transported inwards by the flow. The predicted peak soot volume fraction of 10.3 ppm of the baseline flame, Fig. 2(a), is somewhat higher than the experimental value of about 8 ppm. The very low concentrations of soot in the centerline region represent a well known drawback of most soot models in the prediction of ethylene diffusion flames.

The effects of adding 10% H_2O to the air stream on flame temperature and soot volume fraction can be seen by comparing Figs. 1(a) and 1(b) and Figs. 2(a) and 2(b). It is clear that the effects are significant with the peak temperature being reduced by more than 90 K and the peak soot volume fraction reduced by almost 47%. Besides the effect on the peak flame temperature, the centerline temperatures are also significantly affected. These net effects consist of contributions from all the four mechanisms mentioned earlier, i.e., dilution, thermal, chemical, and radiative. It is important to understand the relative importance of these four mechanisms.

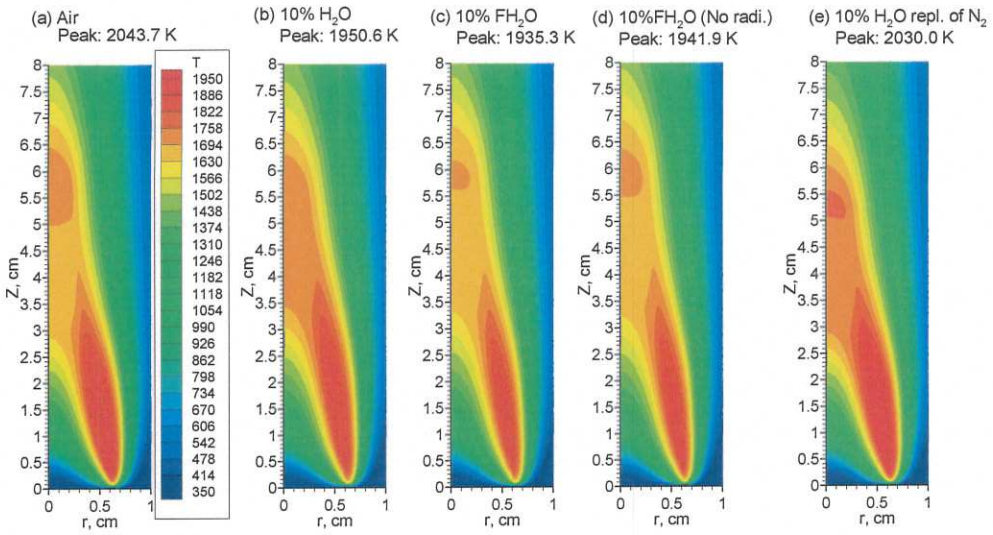

Figure 1. Temperature distributions in the flames without and with 10% H_2O in the oxidizer stream.

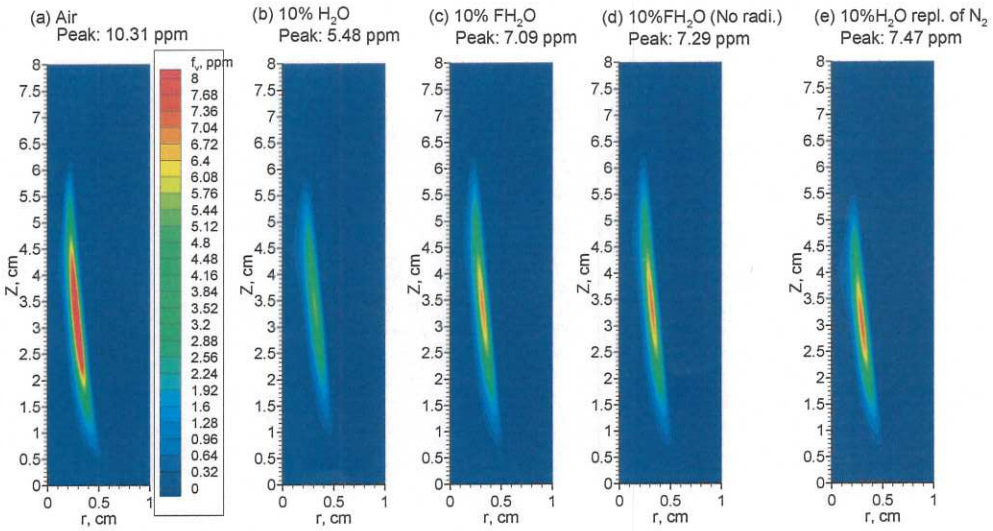

Figure 2. Soot volume fraction distributions in the flames without and with 10% H_2O in the oxidizer stream.

The importance of chemical effect can be assessed by comparing the results shown in Figs. 1(b) and 1(c) for temperature and Figs. 2(b) and 2(c) on soot volume fraction. These results indicate that water vapour does affect the flame temperature and soot formation chemically in a rather significant way. The chemical effect of H_2O increases the flame temperature but lowers soot volume fraction. At 10% H_2O addition the chemical effect increases the peak flame temperature by only about 15 K; however, it increases the centerline temperatures by about 40 K. Meanwhile, the chemical effect of H_2O lowers the peak soot volume fraction by almost 23%. An examination of the reaction rate distributions in Cases 5 and 6 indicates that the primary pathways for the chemical effect of H_2O are the reverse reactions of $OH + H_2 \Leftrightarrow H + H_2O$ (R3) and $OH + OH \Leftrightarrow O + H_2O$ (R4) (in order of decreasing importance). It is worth pointing out that the important role played by reaction of R3 in the chemical effect of water vapour addition has been speculated by Richard et al. [9]. As a

consequence of the active chemical participation of the added water vapour, O and H radical concentrations decrease while OH radical and molecular hydrogen (H_2) concentrations increase. The increased OH radical concentrations enhance the conversion of CO to CO_2 in the centerline region of the flame. This is why the flame temperatures in the upper part of the centerline region are about 40 K higher when the chemical effect of H_2O is accounted for, comparing Figs. 1(b) and 1(c). The higher OH radical concentrations also enhance soot oxidation, leading to a shorter visible flame height, comparing Figs. 2(b) and 2(c). The reduced soot volume fractions due to the chemical effect of the added H_2O are the result of two different chemical actions of H_2O. The first action is the enhanced soot oxidation due to the higher OH radical concentrations. The second one is related to the chemical effect of H_2O on soot inception and surface growth. The chemical effect of the added H_2O reduces the concentrations of A4 in the annular region above the burner rim, leading to lower soot inception rates low in the flame. The reduced H radical concentration implies that the soot surface growth rate is reduced. According to the HACA mechanism, the key reactions in the soot surface reaction sequence are the H-abstraction reaction to form active sites $C_{soot}\text{-H} + H \Leftrightarrow C_{soot\bullet} + H_2$ and the acetylene addition reaction to the active sites, i.e., $C_{soot\bullet} + C_2H_2 \Rightarrow C_{soot}\text{-H} + H$. Although the H-abstraction reaction is reverse, the reverse reaction rate is much lower than the forward one. Therefore, the reduced H radical concentration produces less active site, which in turn results in lower overall soot surface growth rates. The combined actions of the chemical effect of H_2O on soot inception, surface growth, and oxidation lead to significant decrease in soot volume fraction.

The influence of oxygen dilution on the fields of temperature and soot volume fraction can be largely seen by comparing Figs. 1(a) and 1(d) and Figs. 2(a) and 2(d), though the differences between these results also contain the thermal effect of H_2O due to its different heat capacity from that of nitrogen. As expected, this mechanism contributes to decrease the temperatures, resulting in a reduction in soot formation rates. Consequently, lower soot volume fractions are expected. This is indeed the case and the effect of dilution is actually very significant, since it lowers the peak flame temperature by about 100 K (from 2043.7 K to 1941.9 K) and the peak soot volume fraction by about 30% (from 10.31 ppm to 7.29 ppm). A better way to illustrate the effect of dilution is to compare the results shown in Figs. 1(b) and 1(e) for temperature and Figs. 2(b) and 2(e) for soot volume fraction. Again, the dilution effect is seen very significant, which lower the peak temperature by about 80 K and soot volume fraction by about 27%. The dilution effect is the most significant mechanism in affecting the flame temperatures and soot formation.

The radiative effect of the added H_2O to the oxidizer stream can be isolated by comparing the results shown in Figs. 1(c) and 1(d) for flame temperature and Figs. 2(c) and 2(d) for soot volume fraction, though it is recognized that such a comparison is made without the chemical effect of the added H_2O. It is evident that the radiative effect of the added H_2O lowers the flame temperatures and soot volume fraction, though the effect in this small scale laminar diffusion flame is fairly weak. At 10% H_2O addition, the radiative effect of H_2O lowers the peak flame temperature by only about 6 K and the peak soot volume fraction by just under 3%.The radiative effect of H_2O has a more significant influence on the temperatures in the centerline region close to the flame tip where it lowers the temperatures by about 12 K. As discussed earlier, the added H_2O enhances radiative heat loss by increasing the emission from the high temperature regions and also by increasing the radiative absorption of the cold surroundings. It is expected that the radiative effect of the added water vapour becomes more significant in large-scale flames, such as pool fires.

Cross-section area integrated soot volume fraction The flame cross section integrated soot volume fraction distributions without and with 10% H_2O in the oxidizer stream along the height above the burner exit are compared in Fig. 3. It is interesting to observe from this figure that the effect of adding 10% H_2O to the oxidizer stream has almost no influence on the integrated soot

volume fraction at heights above z = 4.3 cm when the chemical effect of H_2O is removed, though the amount of soot is still reduced at heights lower than z = 4.3 cm. These results seem to indicate that the dilution and thermal effects of the added H_2O mainly affect soot inception and surface growth, but not oxidation. On the other hand, when the chemical effect of H_2O is accounted for, the integrated soot distribution is reduced at all heights and soot disappears at a lower height. These results are consistent with those shown in Figs. 2(b) and 2(e), where the chemical effect of H_2O is included and the visible flame heights are shorter. It is also noticed from Fig. 3 that the peak integrated soot volume fraction occurs at a higher flame height with 10% H_2O or FH_2O added to the oxidizer stream. The importance of various effects of the added water vapour to the oxidizer stream on the integrated soot volume fraction is also indicated in Fig. 3. Based on results shown in Fig. 3 and the above discussion related to the dilution effect of H_2O it can be concluded that the order of importance of the various effects of H_2O addition to the oxidizer stream of the laminar coflow ethylene diffusion flame is dilution, chemical, thermal, and radiative.

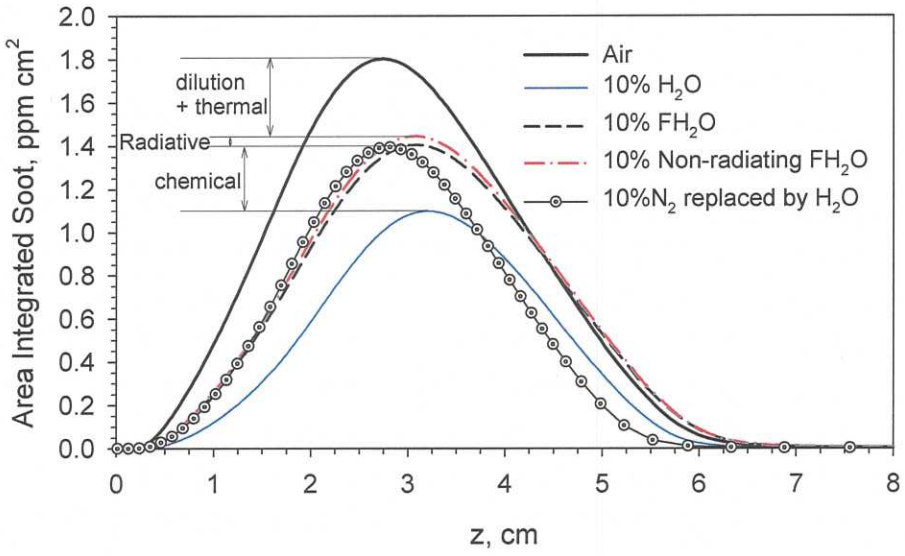

Figure 3. Distributions of the cross section area integrated soot volume fraction without and with 10% H_2O in the oxidizer stream.

Radiant Fraction Radiative losses are quantified by the radiant fraction, χ_R, defined as the fraction of the Heat Release Rate (HRR) radiated from the flame. In this study, the radiant fractions were calculated from the total radiative loss rate (the summation of the product of each control volume and the local radiation source term) and the total combustion HRR (the summation of the product of each control volume and the local heat release rate). The results are summarized in Table 2. For the baseline case, the calculated radiant fraction of 25.82% is in reasonable agreement with that of 22.66% predicted from the experimental correlations of Markstein [27]:

$$\chi_R = 2.0274\times10^{-4}\left(T_{ad}-1087\right)\left(\frac{\dot{Q}}{\dot{Q}_{SP}}\right)^{0.5} \quad (1)$$

where T_{ad}, $\dot{Q}$, and $\dot{Q}_{sp}$ are the adiabatic flame temperature for ethylene/air mixtures taken as 2378K, the HRR, the HRR at the smoke point taken as 212W [28]. It is clear from Table 2 that the reduction in both temperature and soot volume fraction due to the addition of H_2O to the oxidizer stream leads to lower χ_R, comparing Cases 2 and 5 to Case 1. The reductions are about 6.5% and 15% with 5% and 10% H_2O added to the oxidizer stream, respectively. These results also indicate that it is more effective to reduce χ_R by adding water vapour to the oxidizer stream than by nitrogen replacement, comparing Cases 5 and 8 to Case 1.

Table 2: Radiant fraction for the eight flames studied.

	Case 1	Case 2	Case 3	Case 4	Case 5	Case 6	Case 7	Case 8
χ_R (%)	25.82	24.14	25.51	25.84	21.94	24.34	25.00	24.85

CONCLUSIONS

The effects of adding water vapour to the oxidizer stream on flame temperature and soot formation in a laminar coflow ethylene/air diffusion flame were numerically investigated by employing detailed gas-phase chemistry, an advanced soot formation model based on PAH collision and HACA surface reaction mechanisms, and a non-grey gas radiation model. Eight cases were investigated to isolate the dilution, thermal, chemical, and radiative effects of water vapour. Numerical results show that water vapour has a strong chemical effect and a weak radiative effect in this laminar flame. The primary pathways for the chemical effect of water vapour are the reverse reaction of $OH + H_2 \Leftrightarrow H + H_2O$ and $OH + OH \Leftrightarrow O + H_2O$. The chemical effect of water vapour results in higher flame temperatures but lower soot volume fractions. The chemical effect of water vapour affects soot inception, surface growth, and oxidation. The dilution and thermal effects of water vapour mainly reduces soot loading through soot inception and surface growth. In the laminar diffusion flame investigated in this study the order of importance of the four mechanisms of water vapour addition to the oxidizer stream was found to be dilution, chemical, thermal, and radiative. Addition of water vapour to the oxidizer stream is also an effective way to lower radiation heat loss from the flame.

ACKNOWLEDGEMENTS

Dr. Fengshan Liu would like to thank Dr. Prateep Chatterjee and his colleagues of FM Global for useful discussions on issues in fire extinction using water mist.

REFERENCES

1. D. Zhao, H. Yamashita, K. Kitagawa, N. Arai, and T. Furuhata, "Behavior and Effect on NOx Formation of OH Radical in Methane-Air Diffusion Flame with Steam Addition", *Combust. Flame*, vol. 130, pp 352-360, 2002.
2. M. Psota, W. Easley, T. Fort, and A. Mellor, "Water Injection Effects on NOx Emissions for Engines Utilizing Diffusion Flame Combustion", SAE Technical Paper 971657, 1997, doi:10.4271/971657.
3. C. C. Ndubizu, R. Ananth, P. A. Tatem, and V. Motevalli, "On Water Mist Fire Suppression Mechanisms in a Gaseous Diffusion Flame", *Fire Safety J.*, vol. 31, pp 253-276, 1998.
4. R. Ananth, and R. C. Mowrey, "Ultra-Fine Water Mist Extinction Dynamics of a Co-Flow Diffusion Flame", *Combust. Sci. and Tech.*, vol. 180, pp 1659-1692, 2008.
5. A. M. Lentati, and H. K. Chelliah, "Dynamics of Water Droplets in a Counterflow Field and Their Effect on Flame Extinction", *Combust. Flame*, vol. 115, pp 158-179 (1998).
6. A. M. Lentati, and H. K. Chelliah, "Physical, Thermal, and Chemical Effects of Fine-Water Droplets in Extinguishing Counterflow Diffusion Flame", *Proc. Combust. Inst.*, vol. 27, pp 2839-2846, 1998.
7. B. Z. Dlugogorski, R. K. Hichens, E. M. Kennedy, and J. W. Bozzelli, "Propagation of Laminar Flames in Wet Premixed Natural Gas-Air Mixtures", *Trans IChemE*, vol. 76, Part B, pp 81-89, 1998.
8. K. Müller-Dethlefs, and A. F. Schlader, "The Effect of Steam on Flame Temperature, Burning Velocity and Carbon Formation in Hydrocarbon Flames", *Combust. Flame*, vol. 27, pp 205-215, 1976.

9. J. Richard, J. P. Garo, J. M. Souil, J. P. Vantelon, and V. G. Knorre, "Chemical and Physical Effects of Water Vapor Addition on Diffusion Flames", *Fire Safety J.*, vol. 38, pp 569-587, 2003.
10. K. Prasad, C. Li, K. Kailasanath, C. Ndubizu, R. Ananth, and P. A. Tatem, "Numerical Modeling of Water Mist Suppression of Methane-Air Diffusion Flames", *Combust. Sci. Tech.*, vol. 132, pp 325-364, 1998.
11. J. Suh, and A. Atreya, "The Effect of Water Vapor on Counterflow Diffusion Flames", Proceedings of the International Conference on Fire Research and Engineering, D. Peter and E. A. Angell (eds.), September 10-15, 1995, Orlando, FL.
12. C. C. Tseng, and R. Viskanta, "Enhancement of Water Droplet Evaporation by Radiation Absorption", *Fire Safety J.*, vol. 41, pp 236-247, 2006.
13. W. Yang, T. Parker, H. D. Ladouceur, and R. J. Kee, "The Interaction of Thermal Radiation and Water Mist in Fire Suppression", *Fire Safety J.*, vol. 39, pp 41-66, 2004.
14. J.L. Consalvi, B. Porterie, and J.C. Loraud, "Dynamic and Radiative Aspects of Fire/Water Mist Interactions", *Combust. Sci. Technol.*, vol.176, pp. 721-752, 2004.
15. Ö. L. Gülder, D. R. Snelling, and R. A. Sawchuk, "Influence of Hydrogen Addition to Fuel on Temperature Field and Soot Formation in Diffusion Flames", *Proc. Combust. Inst.*, vol. 26, pp 2351-2357, 1996.
16. H. Guo, F. Liu, G. J. Smallwood, and Ö. L. Gülder, "Numerical Study on the Influence of Hydrogen Addition on Soot Formation in a Laminar Ethylene-Air Diffusion Flame", *Combust. Flame*, vol. 145, pp 324-338, 2006.
17. F. Liu, H. Guo, and G. J. Smallwood, "Effects of Radiation Model on the Modelling of a Laminar Coflow Methane/Air Diffusion Flame", *Combust. Flame*, vol. 138, pp 136-154, 2004.
18. F. Liu, and G. J. Smallwood, "An Efficient Approach for the Implementation of the SNB based Correlated-k Method and Its Evaluation", *JQSRT*, vol. 84, pp 465-475, 2004.
19. Q. Zhang, H. Guo, F. Liu, G. J. Smallwood, and M. J. Thomson, "Modeling of Soot Aggregate Formation and Size Distribution in a Laminar Ethylene/Air Coflow Diffusion Flame with Detailed PAH Chemistry and an Advanced Sectional Aerosol Dynamics Model", *Proc. Combust. Inst.*, vol. 32, pp 761-768, 2009.
20. J. Appel, H. Bockhorn, and M. Frenklach, "Kinetic modeling of soot formation with detailed chemistry and physics: laminar premixed flames of C2 hydrocarbons", *Combust. Flame*, vol. 121, pp 122-136, 2000.
21. M. Frenklach, and H. Wang, in: H. Bockhorn (ed.), *Soot Formation in Combustion: Mechanism and Models*, Springer, Berlin, p 165, 1994.
22. S. H. Park, S. N. Rogak, W. K. Bushe, J. Z. Wen, and M. J. Thomson, "An Aerosol Model to Predict Size and Structure of Soot Particles", *Combust. Theory Model.* vol. 9, pp 499-513, 2005.
23. S. V. Patankar, *Numerical Heat Transfer and Fluid Flow*, Hemisphere, New York, 1980.
24. Z. Liu, C. Liao, C. Liu, and S. McCormick, "Multigrid Method for Multi-Step Finite Rate Combustion", AIAA paper 95-0205, 1995.
25. R. J. Kee, F. M. Rupley, and J. A. Miller, "Chemkin-II: A Fortran Chemical Kinetics Package for the Analysis of Gas-Phase Chemical Kinetics", Sandia Report SAND89-8009, Sandia National Laboratory, 1989.
26. Q. Zhang, H. Guo, F. Liu, G. J. Smallwood, and M. J. Thomson, "Implementation of a Fixed Sectional Aerosol Dynamics Model with Soot Aggregate Formation in a Laminar Axisymmetric Coflow Methane/Air Diffusion Flame", *Combust. Theory Model.*, vol. 12, pp 621-641, 2008.
27. G.H. Markstein, "Correlation for smoke points and radiant emission of laminar hydrocarbon diffusion flames", *Proc. Combust. Inst.*, vol. 22, pp. 363-370, 1988.
28. A. Tewarson, "Prediction of Fire Properties of Materials-Part I: Aliphatic and Aromatic Hydrocarbons and Related Polymers", Factory Mutual Research Corporation J.I 0K3R3.RC: (NBS Grant #60NANB4D-0043), 1986.